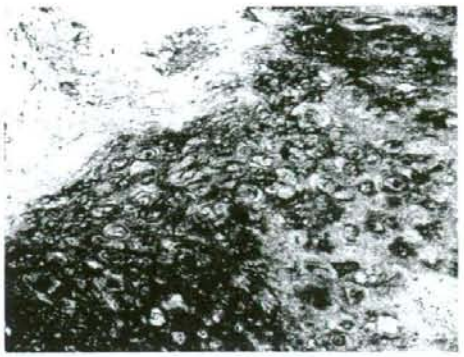

Fig. 1 Pathological specimen from the first operation. The diagnosis is chondrosarcoma (HE. ×200).

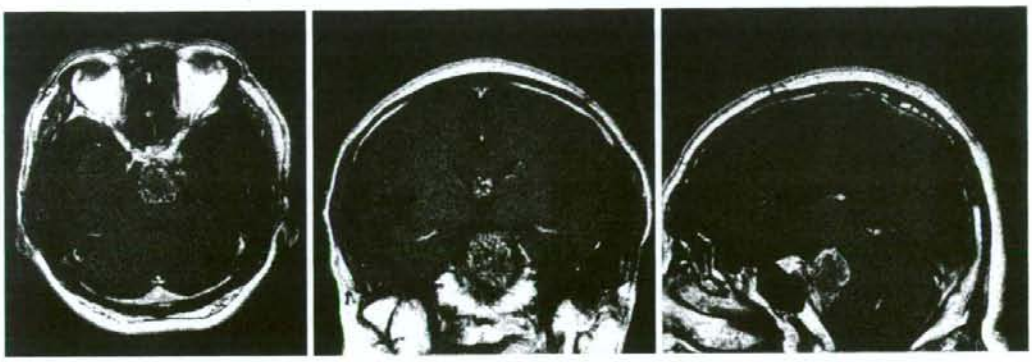

Fig. 2 MRI (T1-Gd enhanced) 33 months after the first operation. The residual tumor is regrowing.

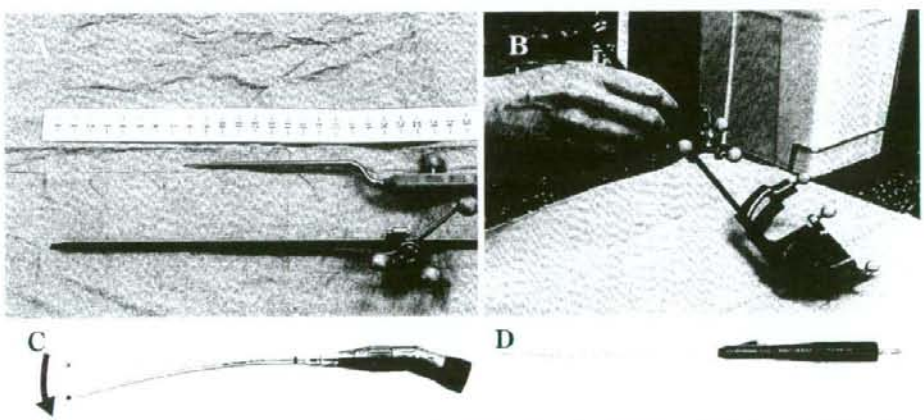

Fig. 3 An original long navigation pointer (**A**) registered by the Universal Instrument Integration system (**B**: VectorVision® : BrainLAB Co.,Ltd.) for this operation. Long and slim instruments we used for this operation, Primado® (**C**: Nakanishi Co.,Ltd.) and SONOPET® (**D**: M & M Co.,Ltd.).

Fig. 4 Intraoperative photograph. Basilar artery (*), capule of tumor (#), and forceps (+).

症例提示

患　者：56歳，男性

主　訴：複視

既往歴：特記事項なし

現病歴：2002年より左方視時の複視を自覚するも放置していた．翌年3月に近医で眼精疲労と診断されていた．2004年8月時点でも症状の改善を認めず，原因検索のため頭部MRIを施行され，頭蓋内病変を指摘，当科紹介となった．

入院時現症：意識はJapan Coma Scale：0．神経学的所見としては左の外転神経麻痺を認めた．

神経放射線学的所見：術前の頭部MRI(T1-Gd)では，トルコ鞍から斜台にかけて後方に突出し，内部が不均一に増強される最大径2.5 cmの腫瘍を認めた．橋は腫瘍により後方に強く圧排され，脳底動脈は右方に偏移していた．

第1回手術：斜台部chondrosarcomaの術前診断の下，2003年3月，Lt. subtemporal approachで摘出術を行った．手術は，ニューロナビゲーションにて腫瘍を確認しながら摘出を行い，右側に圧排された脳底動脈が確認できたところで摘出終了とした．腫瘍の病理診断は，術前診断どおりchondrosarcomaであった（**Fig. 1**）．

第1回術後経過：術後MRIでは残存腫瘍は内減圧されており，今後腫瘍が縮小し脳幹の減圧が期待されるため，後療法は行わず，自宅退院し経過観察となった．その後，およそ4カ月ごとにMRIによる経過観察を行ったが，術後33カ月目のMRIで，明らかな腫瘍の再増大を認めた．

第2回手術：再発腫瘍は側方進展が少なく，後方進展が主体であったため，第2回手術は内視鏡下経鼻経蝶形骨洞手術で行うこととした（**Fig. 2**）．

手術にはOLYMPUS社製の4 mmの0度，30度，70度の視野角を持つ硬性内視鏡と，BrainLAB社製のニューロナビゲーションシステム（VectorVision®）を用いた．また通常のナビゲーション用ポインターは，本症例のように斜台より後方に進展する腫瘍の手術には短いため，任意の手術器械をナビゲーションポインターとして使用できるナビゲーションシステム付属のUniversal Instrument Integrationを用いて長いポインターを自作して使用した．さらに，狭い空間での斜台の掘削，斜台後方の腫瘍摘出のため，細径で長い経鼻手術用に開発されたハイスピードドリル（Primado®：ナカニシ社製），ラパロスコープ用の超音波手術器（SONOPET®：エムアンドエム社製）などの手術機器を用いた（**Fig. 3**）．

第2回手術所見：蝶形骨洞前壁をdrill outし，蝶形骨内に進入すると，蝶形骨洞内に両側の内頸動脈隆起，トルコ鞍が確認された．また，それら3つの構造物に囲まれた斜台の骨は，腫瘍により一部破壊されていた．その部分をナビゲーションシステムにて確認し，これら重要構造物を傷つけないように開窓した．

腫瘍はもろく，出血も少なく，超音波手術器で容易に吸引可能であった．自作したポインターで摘出深度を確かめながら摘出を進め，脳底動脈を避けながら橋の前面まで到達し，クモ膜が摘出腔に下垂してきたところで摘出終了とした（**Fig. 4**）．摘出後，蝶形骨洞内を脂肪とフィブリン糊で充填し，手術を終了した．

第2回術後経過：第2回術後のMRIでは，斜台左上方部分に残存腫瘍が認められた．この部分は，今回用いた下垂体腫瘍に用いる硬性鏡の長さでは短く，視野角のついた内視鏡であってもblindとなる部分であった（**Fig. 5**）．術後は，新たな神経脱落症状，髄液漏などの合併症もなく，自宅独歩退院し，現在も外来にて画像による経過観察を行っており，腫瘍増大時には定位放射線照射を行う予定である．

考　察

斜台部腫瘍に対する手術アプローチには，種々のものが報告されているが[1][7][9]，腫瘍の側方進展が少ない場合，transsphenoidal approachは考慮されるべきアプローチである[5]．

斜台部腫瘍に対するtranssphenoidal approachは，古くは1966年のBoucheらの報告[2]にさかのぼることができるが，当時の手術顕微鏡では側方の視野が確保できず，摘出に限界があり，斜台部腫瘍に対するtranssphenoidal approachは普及しなかった．しかしながら，近年の神経

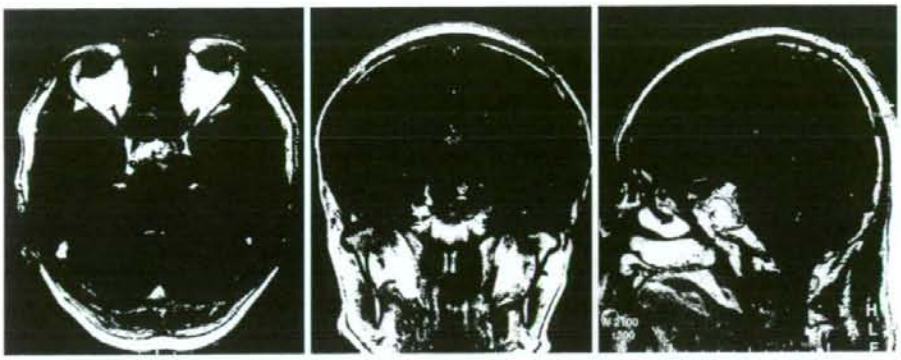

Fig. 5 MRI (T1-Gd enhanced) after the second operation. The remaining tumor was shown in the left superior portion. It seems to be a blind corner with the endoscope that we use, because the endoscope is too short to see there.

内視鏡の発達とともに，広い視野が確保され，摘出率が向上し，手術アプローチとして再評価されるようになった[8]．さらに今回症例で明らかとなったごとく，細径のドリルや超音波手術装置といった手術器械や，ニューロナビゲーションシステムといった最新の技術を応用することによって，より安全，確実に腫瘍摘出術が可能となった．今後，ますます斜台部腫瘍に対する内視鏡下経蝶形骨洞手術の適応が拡大するものと考えられる．ただし，今回の症例の経験から得られた問題点としては，現在トルコ鞍部の手術に用いられている硬性内視鏡では，斜台部後方に存在する腫瘍を側視鏡でみるには短く，blind となり摘出しきれない部位があることが明らかとなった（**Fig. 6**）．今回用いた内視鏡は，脳用の有効長 155～160 mm，外径 4 mm のものであるが，例えば婦人科用としては有効長 280 mm，外径 3 mm のものも存在することから，有効長の長い内視鏡の開発は技術的には可能と考えられ，脳用の 160 mm を超える内視鏡の開発が必要である．また今回使用した超音波吸引器は，先端がまっすぐであるために直視下の腫瘍の摘出には効果を発揮するが，側方の腫瘍の摘出には限界がある．これは顕微鏡下の手術においても同様であり，内視鏡によって側方の視野がより確保されたとしても，側方に存在する腫瘍を摘出するための器材の開発も今後の課題である．

斜台部腫瘍摘出術に際しては，髄液漏が最も危惧される[3)6)10)]．斜台部腫瘍に対する内視鏡下経蝶形骨洞手術の報告は少ないが，Frank らの報告[5)]によると，chordoma, chondrosarcoma に対して内視鏡下経蝶形骨洞手術を行い，髄液漏は 11 例中 2 例（18%）に認めたのみで，その 2 例もフィブリン糊と脂肪組織の充填により治癒していることから，通常のトルコ鞍部の腫瘍摘出と同様の手技で髄液漏のコントロールは可能であると考えられる．しかしこの部位の腫瘍摘出に関して，髄液漏は最終的な手術の成否を分ける重要な合併症であり，症例によっては積極的な腰椎ドレナージの利用や，fascia を用いた硬膜の形成など，症例ごとに十分な髄液漏防止についての検討が必要なのはいうまでもない．また 11 例中 1 例（9 %）に腫瘍摘出時の内頸動脈損傷による出血を認めたと報告しているが，これは不用意にモノポーラ凝固装置を用いた結果とされており，ニューロナビゲーションシステムで内頸動脈を十分確認することで回避可能であったと推測され，術中の出血もコントロール可能な症例が多いと考えられる．内視鏡手術においては，止血方法が問題とされることが多いが，本論文からは，斜台部の chordoma, chondrosarcoma は出血が少なく，内視

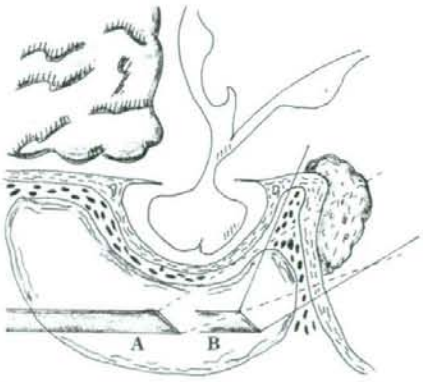

Fig. 6 Illusration showing the difference of range of the endoscopic visual field due to its lengths. **A** is the length we used this time. **B** is the ideal length.

鏡手術のよい適応であると考えられる．今回の症例も出血が少なく，止血操作に難渋することはなかった．このように，側方進展の少ない斜台部の chordoma，chondrosarcoma は，内視鏡下経蝶形骨洞手術のよい適応疾患と考えられた．

結　語

Clival chondrosarcoma の内視鏡下経鼻経蝶形骨洞手術に際して，われわれが行った手術手技の工夫について報告した．内視鏡手術用に開発された手術機器とナビゲーションシステムの応用により，斜台部腫瘍を安全に摘出することができた．侵襲度が高い手術アプローチが多い斜台部腫瘍に対して，より低侵襲な内視鏡下経蝶形骨洞手術の適応拡大が期待される．

問題点としては，斜台部後上方や後下方に進展した腫瘍摘出のためには，現在のトルコ鞍部手術用の硬性内視鏡よりも長い内視鏡の開発が必要であると同時に，今後の課題としては，確保した側方視野に存在する腫瘍を摘出するための器械の開発が挙げられる．

文　献

1) Al-Mefty O, Borba LA：Skull base chordomas：A management challenge. *J Neurosurg* **86**：182-189, 1997.
2) Bouche J, Guiot G, Rougerie J, Freche C：The trans-sphenoidal route in the surgical approach to chordoma of the clivus. *Ann Otolaryngol Chir Cervicofac* **83**：817-834, 1966.
3) Colli B, Al-Mefty O：Chordomas of the craniocervical junction：Follow-up review and prognosis factors. *J Neurosurg* **95**：933-943, 2001.
4) de Divitiis E, Cappabrianca P, Cavallo LM：Endoscopic transsphenoidal approach：Adaptability of the procedure to different sellar lesions. *Neurosurgery* **51**：699-705, 2002.
5) Frank G, Sciarretta V, Calbucci F, Farneti G, Mazzatenta D, Pasquini E：The endoscopic transnasal transsphenoidal approach for the treatment of cranial base chondromas and chondrosarcomas. *Neurosurgery* **59**：50-57, 2006.
6) Gay E, Sekhar LN, Rubinstein E, Wright DC, Sen C, Janecka IP, Snyderman CH：Chordomas and chondrosarcomas of the cranial base：Result and follow-up of 60 patients. *Neurosurgery* **36**：887-897, 1995.
7) Hadley MN, Martin NA, Spetzler RF, Sonntag VK：Comparative transoral dural closure techniques：A canine model. *Neurosurgery* **22**：392-397, 1988.
8) Jho HD, Carrau RL, McLaughlin MR, Somaza SC：Endoscopic transsphenoidal resection of a large chondroma in the posterior fossa. *Acta Neurochir (Wien)* **139**：343-347, 1997.
9) Lanzino G, Sekhar LN, Hirsch WL, Sen CN, Pomonis S, Snyderman CH：Chondomas and chondrosarcomas involving the cavernous sinus：Review of surgical treatment and outcome in 31 patients. *Surg Neurol* **40**：359-371, 1993.
10) Maira G, Pallini R, Anile C, Fernandez E, Salvinelli F, La Rocca LM, Rossi GF：Surgical treatment of clival chordomas：The transsphenoidal approach revisited. *J Neurosurg* **85**：784-792, 1996.

要　旨

斜台部腫瘍摘出における経鼻孔内視鏡手術の経験
―術式の工夫―

斎藤　佑規　　土谷　大輔　　櫻田　　香
佐藤　慎哉　　黒木　　亮　　嘉山　孝正

斜台部腫瘍への手術アプローチには種々の方法があるが，前後方向への進展が主体で側方進展が軽度の場合には，経蝶形骨洞手術も選択肢の 1 つである．従来の顕微鏡手術による本アプローチは，術野が狭く，手術アプローチとしては普及しなかった．しかし，近年の神経内視鏡やニューロナビゲーションシステムの発達は，広い術野の確保と周囲の重要構造物の同定に威力を発揮し，経蝶形骨洞手術の斜台部腫瘍への適応が拡大している．今回は，内視鏡下経蝶形骨手術にて摘出術を行った chondrosarcoma の 1 例を経験したので，その手術に際してわれわれが行った技術的工夫と手術における問題点につき報告する．

脳外誌　17：50-54，2008

J Neurooncol (2008) 90:223–228
DOI 10.1007/s11060-008-9654-x

CLINICAL STUDY - PATIENT STUDY

Immunohistochemical profiles of brain metastases from breast cancer

Kan Yonemori · Koji Tsuta · Chikako Shimizu · Yutaka Hatanaka · Kaoru Hashizume · Makiko Ono · Yukihiro Nakanishi · Tadashi Hasegawa · Yasuji Miyakita · Yoshitaka Narita · Soichiro Shibui · Yasuhiro Fujiwara

Received: 25 February 2008 / Accepted: 7 July 2008 / Published online: 23 July 2008

Abstract The aim of present study is to explore the immunohistochemical profiles of brain metastases from breast cancer. We retrospectively performed immunohistochemical staining for estrogen receptor (ER), progesterone receptor (PgR), human epidermal growth factor receptor type 2 (HER2/neu), and cytokeratin (CK) 5/6 in 29 patients with resected tumor specimens of brain metastases. Immunohistochemical staining for ER, PgR and HER2/neu was performed in 24 patients with primary tumors. The positive frequency of immunohistochemical profiles of ER, PgR, HER2/neu, and CK5/6, in the brain metastases were 13.8%, 6.9%, 37.9%, and 24.1%, respectively. The immunohistochemical profiles including ER, PgR, and HER2/neu of the primary tumor and the brain metastasis differed in seven patients (29.2%, N = 7/24). Interestingly, the biological characteristics of brain metastasis sometimes changed which were represented by immunohistochemical staining. Therefore, the changes in the biological features of breast cancer should be taken into account when developing treatment strategies, including new molecular-targeted drugs, for brain metastases.

Keywords Immunohistochemical staining · Discordance · Hormone receptor · HER2/neu · Breast cancer · Brain metastasis

K. Yonemori · C. Shimizu · M. Ono · Y. Fujiwara
Breast and Medical Oncology Division, National Cancer Center Hospital, 5-1-1 Tsukiji, Chuo-ku, Tokyo 104-0045, Japan
e-mail: yonemori-kan@pmda.go.jp

K. Tsuta (✉) · Y. Fujiwara
Clinical Laboratory Division, National Cancer Center Hospital, 5-1-1 Tsukiji, Chuo-ku, Tokyo 104-0045, Japan
e-mail: ktsuta@ncc.go.jp

Y. Hatanaka · K. Hashizume
Dako Japan Inc., 2-5-1, Kouraku, Bunkyo-ku, Tokyo 112-0004, Japan

Y. Nakanishi
Pathology Division, National Cancer Center Institute, 5-1-1 Tsukiji, Chuo-ku, Tokyo 104-0045, Japan

T. Hasegawa
Department of Surgical Pathology, Sapporo Medical School of Medicine, South 1 West 16, Chuo-ku, Sapporo, Hokkaido 104-0045, Japan

Y. Miyakita · Y. Narita · S. Shibui
Neurosurgery Division, National Cancer Center Hospital, Tokyo, Japan

Introduction

Brain metastasis is the most common type of malignancy found in the brain and is responsible for a substantial fraction of the total morbidity and mortality of metastatic breast cancer patients. Brain metastasis is generally a late feature in the history of metastatic breast cancer. The incidence of symptomatic brain metastases in metastatic breast cancer ranges from 10% to 16% and has been reported to be even higher in human epidermal growth factor receptor type 2 (HER2/neu)-positive tumors [1]. Current systemic therapy, including hormone therapy, chemotherapy and molecular-targeted drug therapy, is not effective for the treatment of brain metastasis, and the development of treatment strategies for brain metastasis has become a critical issue.

A recent study reported that patients with HER2/neu-positive metastatic breast cancer had a high incidence of subsequent brain metastasis than HER2/neu-negative patients [2–4]. The human epidermal growth factor

receptor family is involved in cell proliferation, differentiation, and survival. HER2/neu amplification is widely known to indicate an aggressive tumor behavior and poor clinical outcome in breast cancer patients. HER2/neu over expression occurs in approximately 20–30% of breast cancer patients [5]. Trastuzumab, a monoclonal antibody against HER2/neu, has been shown to be significantly effective in both adjuvant and metastatic settings [6, 7].

One interpretation of these results was that HER2/neu-positive breast cancer may have a biological affinity toward the development of brain metastasis or trastuzumab-containing therapy prolongs survival until the eventual development of brain metastasis. On the other hand, evidence indicated trastuzumab cannot enter cerebrospinal fluid [8]. Blood brain barrier creates a "sanctuary" for cancer cells where antitumor agents cannot penetrate in high enough concentrations to have any substantial effect. However, whether prolonged patient survival enables cancer cells that have become resistant to trastuzumab to metastasize to the brain remains uncertain. Furthermore, whether brain metastases continue to overexpress HER2/neu and to be sensitive to trastuzumab therapy also remains unknown.

On the other hand, triple negative breast carcinomas (TNBCs) are a group of primary breast tumors with aggressive clinical behavior that account for 10–15% of all breast cancers [9]. Most TNBCs possess a basal phenotype and show varying degrees of basal cytokeratin (CK) and myoepithelial marker expression. Histologically, such cancers are poorly differentiated, and most fall into the basal subgroup of breast cancers, characterized by staining for basal markers (i.e., CK5/6) [10]. A previous study, in which primary tumors were immunohistochemically analyzed, reported that patients with estrogen receptor (ER)-negative and progesterone receptor (PgR)-negative tumors either with or without HER2/neu over-expression had a high risk of brain metastasis in a case-controlled study. A multivariate analysis of a database containing 10,782 patients in another study also reported that the independent risk factors for central nervous system metastasis were ER negativity, a young age, and a histology of invasive ductal carcinoma [11].

We therefore investigated the immunohistochemical profiles, including ER, PgR, HER2/neu, and CK5/6 of brain metastases in breast cancer patients. In addition, we investigated the changes in the immunohistochemical profiles of the primary tumors and the brain metastases.

Patients and methods

Patients

Two hundred fifty-two patients with breast cancer received trastuzumab-based chemotherapy between January 1999 and January 2006 at the National Cancer Center Hospital (NCCH), in Japan. (48 patients in neo-adjuvant setting and 204 patients in metastatic or recurrent setting) Of these, 74 patients (36.3%) developed brain metastases. Twenty-nine patients with brain metastasis were retrospectively identified based on records in the hospital's surgical database. All clinical information was collected from patient chart. Trastuzumab had been initially administered at an intravenous loading dose of 4 mg/kg, followed by weekly infusions of trastuzumab (2 mg/kg) in combination with chemotherapy. The present study was approved by the Institutional Review Board of the National Cancer Center.

Tissue samples and microscopic and immunohistochemical analysis

Hematoxylin–eosin stained specimens were reviewed by two pathologists (K.T. and K.S.) and were confirmed to contain an adequate amount of cancer tissue available for use in the present study. All tumor specimens from brain metastasis resections were available for immunohistochemical analysis. Tumor specimens from primary breast cancers were available for immunohistochemical analysis of ER, PgR, and HER2/neu in 24 of the 29 patients.

The pathological and immunohistochemical examinations were conducted by the same pathologists (K.T. and K.S.), who were blinded to the clinical statuses of the patients. Formalin-fixed, paraffin-embedded tissue samples were sectioned (4-μm thick) and mounted on charged slides. Immunohistochemical staining for ER (clone 1D5; DAKO, Carpinteria, CA), PgR (clone PgR636; Dako), and CK5/6 (clone D5/16B4; Dako) were performed using the streptavidin-biotin method and were considered positive if 10% or more of the nuclei in the invasive component of the tumor were stained [12, 13]. The HER2/neu status, as assessed using Herceptest (Dako), was scored on a scale of 0 to 3+, according to the Dako scoring system. HER2/neu-positive was defined by HER2/neu 3+ or HER2/neu 2+ and fluorescence in situ hybridization-positive. Negative controls, in which the primary antibody was omitted, were also included in each run.

Statistical analysis

The comparisons were made between two groups using a Chi-square test, a Fisher exact test. All the statistical analyses were performed using SPSS 12.0J (SPSS Inc., Chicago, IL, USA), and the significance level for the results was set at 0.05 (two-sided).

Results

The present study included 29 patients with brain metastasis, and the median age at the time of the diagnosis of

Table 1 Patient characteristics

Characteristics of brain metastasis	Prior history of trastuzumab		Total
	(+)	(−)	
Median size (in mm) of brain metastasis (range)	32 (30–40)	36 (20–60)	35 (20–60)
Number of brain metastases			
1	6	18	24
2	2	2	4
3	0	1	1
Side (right/left/bilateral)	1/6/1	13/8/0	14/14/1
Site			
Frontal lobe	0	1	1
Parietal lobe	0	2	2
Temporal lobe	1	5	6
Occipital lobe	1	2[a]	3[a]
Cerebellum	6	10[a]	16[a]

[a] One patient had brain metastases in both the cerebellum and occipital lobe

brain metastasis was 53 years old (range, 39–78 years). The median time to brain metastasis from the time of breast cancer diagnosis was 2.9 years (range, 0–23.1 years).

In this study, eight patients had a prior history of receiving chemotherapy containing trastuzumab, seven of these patients had received trastuzumab-containing chemotherapy in a metastatic setting, and one had received trastuzumab-containing neo-adjuvant chemotherapy, five patients had a prior history of receiving hormone therapy, seven patients had a prior history of receiving chemotherapy, two patients had a prior history of receiving both hormone therapy and chemotherapy, and seven patients had received no systemic therapy prior to the brain tumor resection.

The patient characteristics are shown in Table 1. After the brain tumor resection, most patients (59%) received whole brain radiotherapy, eight patients received local brain radiotherapy, one patient received γ-knife radiotherapy, and three patients did not receive additional brain radiotherapy. After the completion of the local treatment for metastatic brain tumor, 14 patients received systemic chemotherapy, including three patients who received combination chemotherapy including trastuzumab, one patient who received trastuzumab therapy alone, five patients who received hormone therapy, and three patients who received intrathecal chemotherapy because of the rapid progression of meningeal carcinomatosis. Six patients received supportive care alone. The median overall survival time was 14.7 months.

The positive frequency of immunohistochemical profiles of ER, PgR, and HER2/neu, in 24 primary tumors were 12.5% (N = 3/24), 8.3% (N = 2/24), 37.5% (N = 9/24), respectively. The positive frequency of immunohistochemical profiles of ER, PgR, HER2/neu, and CK5/6, in 29 brain metastases were 13.8% (N = 4/29), 6.9% (N = 2/29), 37.9% (N = 11/29), and 24.1% (N = 5/29), respectively (Table 2). Among patients with both hormone-negative and HER2/neu-negative statuses, basal type (CK5/6 positive) breast cancer was observed in 42.9% (N = 6/14). The staining results for ER, PgR, HER2/neu and CK5/6 in the brain metastases were not statistically correlated with a prior history of receiving trastuzumab-containing chemotherapy (Table 2).

Table 2 Relationship between prior history of receiving trastuzumab and immunohistochemical profiles in specimens obtained from brain metastasis (Chi-square test and Fisher exact test)

Variables	Total (%) n = 29	Prior history of trastuzumab		*P*-value
		(+)	(−)	
ER				0.99
Negative	25	7	18	
Positive	4	1	3	
PgR				0.99
Negative	27	8	19	
Positive	2	0	2	
HER2/neu				0.402
Negative	18	2	16	
Positive	11	6	5	
CK5/6				0.99
Negative	22	6	16	
Positive	7	2	5	
Basal type[a]				0.647
No	23	7	16	
Yes	6	1	5	

Abbreviations: ER, estrogen receptor; PgR, progesterone receptor; HER2/neu, human epidermal receptor type 2; NA, not applicable

[a] Basal type in present study defined as ER negative, PgR negative, HER2/neu negative, and CK5/6 positive brain metastasis

The frequencies of immunohistochemical change in ER, PgR, and HER2/neu were 12.5% (N = 3/24), 4.2% (N = 1/24), and 12.5% (N = 3/24), respectively (Table 3). The immunohistochemical profiles for ER, PgR, and HER2/neu differed between the primary tumors and the brain metastases in seven patients (29.2%; N = 7/24, see Table 4). With regard to the systemic treatment options, the treatment options for six patients (25%) were changed based on the immunohistochemical profiles of their brain metastases. Among the patients who had been previously treated with trastuzumab, 25% of the patients (N = 2/8) had changed to a HER2/neu-negative status.

Discussion

The present study demonstrated immunohistochemical characteristics for ER, PgR, HER2 receptor, and CK5/6 of

Table 3 Changes in immunohistochemical profiles in estrogen receptor, progesterone receptor or HER2 receptors between primary tumors and brain metastases (n = 24)

Primary tumor	Brain metastasis	N
ER (−)	ER (−)	19
	ER (+)	*2*[a]
ER (+)	ER (−)	*2*
	ER (+)	1
PgR (−)	PgR (−)	22
	PgR (+)	0
PgR (+)	PgR (−)	*1*
	PgR (+)	1
HER2/neu (−)	HER2/neu (−)	14
	HER2/neu (+)	*1*
HER2/neu (+)	HER2/neu (−)	*2*[a]
	HER2/neu (+)	7

Abbreviations: ER, estrogen receptor; PgR, progesterone receptor; HER2/neu, human epidermal receptor type 2

Italic number indicated seven patients who had changes of immunohistochemical profiles

[a] One patient with an ER-negative, PgR-negative, HER2-positive primary tumor developed an ER-positive, PgR-negative, HER2/neu-negative brain metastasis

Table 4 Discordance cases of immunohistochemical profiles between primary tumor and brain metastasis (N = 7)

Case no.	ER		PgR		HER2/neu	
	Primary	Brain meta	Primary	Brain meta	Primary	Brain meta
1	+	−	−	−	−	−
2	−	−	+	−	−	−
3	+	−	+	−	−	−
4	−	+	−	−	+	+
5	−	−	−	−	−	+
6	−	−	−	−	+	−
7	−	+	−	−	+	−

Abbreviations: ER, estrogen receptor; PgR, progesterone receptor; HER2/neu, human epidermal receptor type 2

brain metastases from breast cancer patients. Although present study had small number of patients and potential selection bias, it is remarkable that the biological characteristics of brain metastasis sometimes changed from the primary tumors.

ER, PgR and HER2/neu immunohistochemical profiles of the primary tumors differed from those of the brain metastases in 29.2% of the patients in the present study; in particular, the HER2/neu status of the two specimens differed in 12.5% of the patients. Generally, marked intratumoral heterogeneity is rare than the degree of heterogeneity (as determined using immunohistochemical analyses and FISH) between primary tumors and their metastases [14–16]. Some previous reports have compared the HER2/neu status of primary tumors and metastases, including axillary lymph node metastasis, local recurrence, distant metastasis, and autopsy findings, but only one study addressed brain metastases. These previous studies, excluding the study that examined brain metastases, described discordance rates of between 0% and 37.5% [14, 16–22]. In a study comparing primary tumors and axillary or metastatic lymph nodes, 0–2% of the patients had a discordance in their HER2/neu statuses [23, 24]. Similar to the results of these studies, discordance has been reported in <5% of primary tumors and their local recurrences [14, 16]. Meanwhile, the rate of discordance in studies examining distant metastasis at various sites was between 6% and 37.5% [17–21]. Among these studies, only two included patients with brain metastasis, but less than five patients were reported and they were not described in detail [17, 18].

Only one study examining patients with brain metastasis reported that 51.5% (N = 17/33) of the patients exhibited the over-expression of HER2/neu (as determined using immunohistochemical analyses) and 25.8% (N = 8/31) exhibited HER2/neu gene amplification. The concordance rate between the immunohistochemical analyses and FISH was 86% when compared with individual metastatic lesions (43 lesions). The concordant rates between the primary tumors and the brain metastases were 58% (N = 7/12) according to the immunohistochemical analyses and 100% (N = 10/10) according to FISH [25]. Although the frequency of discordance between the primary tumors and the brain metastases differed among the studies, probably because of differences in the measurement methods and the small sample sizes, it is important to realize that the brain metastases in some patients have different HER2/neu statuses from those of the primary tumors.

Hormone positivity in the brain metastases was relatively low in this cohort. Hormone receptor discordance in locoregional recurrences or lymph node metastasis may be more frequent than HER2/neu discordance. The rates of discordance have been reported to be 10–25% for ER and 21–44% for PgR between the primary tumor and locoregional recurrence or lymph node metastasis [14, 24, 26, 27]. The rate of discordance between the primary tumor and distant metastasis was similar to that of regional lymph node metastasis or recurrence, which were reported to be 28–42% for ER and 17% for PgR [26, 27]. The discordance rate for hormone receptors in the present study was slightly lower than those reported in previous studies, but whether the hormonal characteristics of brain metastasis differ from those of other distant metastases remains uncertain.

Although the overall frequency of CK5/6 positive brain metastases was low (24.1%, N = 7/29) in present

study, most of patients (71.3%, N = 5/7) were basal type subgroup in patients with CK5/6 positive brain metastases. A previous study revealed that primary tumors which were negative for ER but that expressed basal CK5/6 and overexpressed HER1 or HER2/neu were more likely to develop brain metastasis [28]. The changes in basal type markers between the primary tumors and the brain metastases are uncertain in the present study because CK5/6 staining was not performed in the primary tumors.

There is one report that suggests chemotherapy do not modify the HER2/neu status in metastatic lesions [16]. On the other hand, Regitnig et al. reported that HER2/neu amplification and overexpression may occur de novo in distant metastasis at a late stage of disease [18]. Currently, possible mechanisms of trastuzumab-resistance include the down-regulation of p27, the activation of insulin-like growth factor receptor (IGF-1R), the loss of PTEN, pAkt, interactions between HER family members, the masking of HER2/neu by membrane-associated glycoprotein mucin-4, angiogenesis, and the induction of antibody-dependent cellular toxicity by the immune system [29, 30]. These hypotheses remain controversial, and some studies assessing IGF-1R and p53 in clinical samples have reported negative results [12, 31]. Our study suggests that some patients with HER2/neu negative primary whose brain metastasis were HER2/neu positive responded to trastuzumab therapy after diagnosis of brain metastasis [21]. However, whether the biological changes in the breast cancer cells described in the present study and in previous studies influence the mechanism of resistance to trastuzumab therapy remains unknown.

The present results suggest that all distant metastases should not be assumed to be biologically equal to locoregional metastasis, and that a re-assessment of the immunohistochemical status of the brain metastasis, if possible, may be useful to optimize treatment. Further studies are warranted to address the reason of discordance in the immunohistochemical profiles of the primary tumors and the brain metastases.

Acknowledgements This study was supported by grants from the Ministry of Health, Labour, and Welfare. The authors thank Kunihiko Seki, M.D. (Clinical Laboratory Division, National Cancer Center Hospital), Eriko Nakano, M.D., Mayu Yunokawa, M.D., Tsutomu Kouno, M.D., Masashi Ando, M.D., Noriyuki Katsumata, M.D., and Kenji Tamura, M.D., PhD. (Breast and Medical Oncology Division, National Cancer Center Hospital) for their assistance.

References

1. Lin N, Bellon J, Winer E (2004) CNS metastases in breast cancer. J Clin Oncol 22:3608–3617. doi:10.1200/JCO.2004.01.175
2. Clayton AJ, Danson S, Jolly S et al (2004) Incidence of central metastasis in patients treated with trastuzumab for metastatic breast cancer. Br J Cancer 91:639–643
3. Gabos Z, Sinha R, Hanson J et al (2006) Prognostic significance of human epidermal growth factor receptor positivity for the development of brain metastasis after newly diagnosed breast cancer. J Clin Oncol 24:5658–5663. doi:10.1200/JCO.2006.07.0250
4. Matsumoto K, Shimizu C, Fujiwara Y (2006) The next step to approaching central nervous system metastasis in HER-2-positive metastatic breast patients. Asia Pac J Clin Oncol 2:6–8. doi:10.1111/j.1743-7563.2006.00044.x
5. Slamon DJ, Clark GM, Wong SG et al (1987) Human breast cancer: correlation of relapse and survival with amplification of HER2/neu oncogene. Science 235:177–182. doi:10.1126/science.3798106
6. Slamon DJ, Leyland-Jones B, Shak S et al (2001) Use of chemotherapy plus a monoclonal antibody against HER2 for metastatic breast cancer that overexpresses HER2. N Engl J Med 344:783–792. doi:10.1056/NEJM200103153441101
7. Piccart-Gebhart MJ, Proctor M, Leyland-Jones B et al (2005) Trastuzumab after adjuvant chemotherapy in HER2-positive breast cancer. N Engl J Med 353:1659–1672. doi:10.1056/NEJMoa052306
8. Pestalozzi BC, Brignoli S (2000) Trastuzumab in CSF. J Clin Oncol 18:2349–2351
9. Cleator S, Heller W, Coombes RC (2007) Triple-negative breast cancer: therapeutic options. Lancet Oncol 8:235–244. doi:10.1016/S1470-2045(07)70074-8
10. Nielsen TO, Hsu FD, Jensen K et al (2004) Immunohistochemical and clinical characterization of the basal like subtype of invasive breast carcinoma. Clin Cancer Res 10:5367–5374. doi:10.1158/1078-0432.CCR-04-0220
11. Tham YL, Sexton K, Kramer R et al (2006) Primary breast cancer phenotypes associated with propensity for central nervous system metastases. Cancer 107:696–704. doi:10.1002/cncr.22041
12. Perren A, Weng L-P, Boag AH et al (1999) Immunohistochemical evidence of loss of PTEN expression in primary ductal adenocarcinoma of the breast. Am J Pathol 155:1254–1260
13. Harvey JM, Clark G, Ml Osborne CK et al (1999) Estrogen receptor status by immunohistochemistry is superior to the ligand-biding assay for predicting response to adjuvant endocrine therapy in breast cancer. J Clin Oncol 17:1474–1481
14. Shimizu C, Fukutomi T, Tsuda H et al (2000) c-erbB-2 Protein overexpression and p53 immunoreaction in primary and recurrent breast cancer tissues. J Surg Oncol 73:17–20. doi:10.1002/(SICI)1096-9098(200001)73:1<17::AID-JSO5>3.0.CO;2-2
15. Pertschuk LP, Axiotis CA, Feldman JG et al (1999) Marked intratumoral heterogeneity of the proto-oncogene Her-2/neu determined by three different detection systems. Breast J 5:369–374. doi:10.1046/j.1524-4741.1999.97088.x
16. Gong Y, Booser DJ, Sneige N (2005) Comparison of HER-2 status determined by fluorescence in situ hybridization in primary and metastatic breast carcinoma. Cancer 103:1763–1769. doi:10.1002/cncr.20987
17. Gancberg D, Di Leo A, Cardoso F, Rouas G, Pedrocchi M, Paesmans M et al (2002) Comparison of HER2-status between primary breast cancer and corresponding distant metastatic sites. Ann Oncol 13:1036–1043. doi:10.1093/annonc/mdf252
18. Regitnig P, Schippinger W, Lindbauer M, Samonigg H, Lax SF (2004) Change of HER2/neu status in a subset of distant metastases from breast carcinomas. J Pathol 203:918–926. doi:10.1002/path.1592
19. Pectasides D, Gaglia A, Arapantoni-Dadioti P, Bobota A, Valavanis C, Kostopoulou V et al (2006) Her2/neu status of primary breast cancer and corresponding metastatic sites in patients with advanced breast cancer treated with trastuzumab-based therapy. Anticancer Res 26:647–654

20. Lower EE, Glass E, Blau R, Harman S (2008) Her-2/neu expression in primary and metastatic breast cancer. Breast Cancer Res Treat. doi:10.1007/s10549-008-9931-6
21. Zidan J, Dashkovsky I, Stayerman C, Basher W, Cozacov C, Hadary A (2005) Comparison of HER2/neu overexpression in primary breast cancer and metastatic sites and its effect on biological targeting therapy of metastatic disease. Br J Cancer 93:552–556. doi:10.1038/sj.bjc.6602738
22. Niehans GA, Singleton TP, Dykoski D, Kiang DT (1993) Stability of HER-2/neu expression over time and at multiple metastatic sites. J Natl Cancer Inst 85:1230–1235. doi:10.1093/jnci/85.15.1230
23. Cardoso F, Di Leo A, Larsimont D, Gancberg D, Rouas G, Dolce S et al (2001) Evaluation of HER2, p53, bcl-2, topoisomerase II-alfa, heat shock proteins 27 and 70 in primary breast cancer and metastatic ipsilateral axillary lymph nodes. Ann Oncol 12:615–620. doi:10.1023/A:1011182524684
24. Tsutsui S, Ohno S, Murakami S, Kataoka A, Kinoshita J, Hachitanda Y (2002) EGFR, c-erbB2, and p53 protein in the primary lesions and paired metastatic regional lymph nodes in breast cancer. EJSO 28:383–387. doi:10.1053/ejso.2002.1259
25. Lear-Kaul KC, Yoon HR, Kleinschmidt-DeMasters BK et al (2003) HER2/neu status in breast cancer metastases to the central nervous system. Arch Pathol Lab Med 127:1451–1457
26. Kamby C, Rasmussen BB, Kristensen B (1989) Oestrogen receptor status of primary breast carcinomas and their metastases. Relation to pattern of spread and survival after recurrence. Br J Cancer 60:252–257
27. Li BD, Byskosh A, Molteni A, Duda RB (1994) Estrogen and progesterone receptor concordance between primary and recurrent breast cancer. J Surg Oncol 57:71–77. doi:10.1002/jso.2930570202
28. Hicks DG, Short SM, Prescott NL et al (2006) Breast cancers with brain metastases are more likely to be estrogen receptor negative, express the basal cytokeratin CK5/6, and overexpress HER2 or EGFR. Am J Surg Pathol 30:1097–1104. doi:10.1097/01.pas.0000213306.05811.b9
29. Mohsin SK, Weiss HL, Gonzarrez MC et al (2005) Neoadjuvant trastuzumab induces apoptosis in primary breast cancers. J Clin Oncol 23:2460–2468. doi:10.1200/JCO.2005.00.661
30. Nagata Y, Lan LH, Zhou X et al (2004) PTEN activation contributes to tumor inhibition by trastuzumab, and loss of PTEN predicts trastuzumab resistance in patients. Cancer Cell 6:117–127. doi:10.1016/j.ccr.2004.06.022
31. Nahta R, Yu D, Hung MC et al (2006) Mechanisms of disease: understanding resistance to HER2-targeted therapy in human breast cancer. Nat Clin Pract Oncol 3:269–280. doi:10.1038/ncponc0509

Image of the Month

Three Cases of Sub-scalp Tumor Presenting with Protrusion of the Head

Case 1 was an 81-year-old male who underwent right nephrectomy for renal cell carcinoma 5 years ago. When he fell down and hit his back of the head, he noticed an occipital lump (Fig. 1). The bulging was growing gradually within several months. He underwent an excisional biopsy and pathological findings showed a metastatic tumor from renal cell carcinoma. Irradiation was administered. Case 2 was a 58-year-old female who suffered head trauma 3 years ago. She noticed a protrusion on her parietal cranium while grooming her own hair (Fig. 2). She received a needle biopsy and the pathological diagnosis was meningioma. She underwent surgical resection of the tumor and cranioplastic surgery. Case 3 was an 81-year-old male who had tingling-numb on his forehead for 6 months. Because of the persistent dysesthesia accompanied by progressive swelling (Fig. 3), he consulted our hospital and was operated on for histological confirmation. Obtained tissues were composed of poorly differentiated carcinoma. He subsequently received irradiation on the frontal lesion.

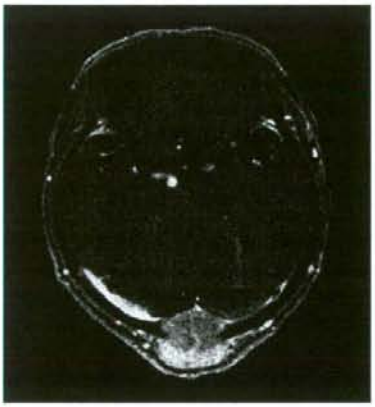

Figure 1.

Figure 2.

Figure 3.

Yasuji Miyakita and Soichiro Shibui
Neurosurgery Division
National Cancer Center Hospital
Tokyo, Japan
doi:10.1093/jjco/hyn023

J Neurosurg 109:811–816, 2008

Transient expansion of vestibular schwannoma following stereotactic radiosurgery

Clinical article

Osamu Nagano, M.D.,[1] Yoshinori Higuchi, M.D., Ph.D.,[1] Toru Serizawa, M.D., Ph.D.,[2] Junichi Ono, M.D., Ph.D.,[3] Shinji Matsuda, M.D.,[4] Iwao Yamakami, M.D., Ph.D.,[1] and Naokatsu Saeki, M.D., Ph.D.[1]

[1]Department of Neurological Surgery, Chiba University Graduate School of Medicine, Chiba; and [2]Gamma Knife House, Departments of [3]Neurosurgery and [4]Neurology, Chiba Cardiovascular Center, Ichihara, Japan

Object. The authors prospectively analyzed volume changes in vestibular schwannomas (VSs) after stereotactic radiosurgery.

Methods. One hundred consecutive patients with unilateral VS treated with Gamma Knife surgery (GKS) at Chiba Cardiovascular Center between 1998 and 2006 were analyzed in this study. For each lesion the Gd-enhanced volume was measured serially every 3 months in the 1st year, then every 6 months thereafter, using volumetric software. The frequency and degree of transient tumor expansion were documented and possible prognostic factors were analyzed. Concurrently, neurological deterioration involving trigeminal, facial, and cochlear nerve functions were also assessed.

Results. The mean observation period was 65 months (range 25–100 months). There were 32 men and 68 women, whose mean age was 59.1 years (range 29–80 years). Tumor volumes at GKS averaged 2.7 cm^3 (range 0.1–13.2 cm^3), and the lesions were irradiated at the mean 52.2% isodose line for the tumor margin (range 50–67%), with a mean dose of 12.2 Gy (range 10.5–13 Gy) at the periphery. The tumor volume was increased by 23% at 3 months and 27% at 6 months. Tumors shrank to their initial size over a mean period of 12 months. The maximum volume increase was < 10% (no significant increase) in 26 patients, 10–30% in 23, 30–50% in 22, 50–100% in 16, and > 100% in 13. The peak tumor expansion averaged 47% (range 0–613%). A high-dose (≥ 3.5 Gy/min) treatment appears to be the greatest risk factor for transient tumor expansion, although the difference did not reach statistical significance. Transient facial palsy and facial dysesthesia correlated strongly with tumor expansion, but only half of the hearing loss was coincident with this phenomenon.

Conclusions. Transient expansion of VSs after GKS was found to be much more frequent than previously reported, strongly suggesting a correlation with deterioration of facial and trigeminal nerve functions.
(DOI: 10.3171/JNS/2008/109/11/0811)

Key Words • **facial nerve function** • **Gamma Knife surgery** • **stereotactic radiosurgery** • **transient tumor expansion** • **trigeminal nerve dysesthesia** • **vestibular schwannoma**

Recently, SRS for small VSs has been established as being efficacious, with high tumor control rates and extremely low incidences of severe complications.[11,18–21,23] However, we occasionally encounter transient cranial neuropathies, such as facial dysesthesia, facial spasm, tinnitus, vertigo, and hearing loss. Typical MR images show initial enlargement with central low intensity within 1 year after treatment, termed "temporary enlargement,"[14] "tumor expansion,"[6,19] or "transient expansion."[4] Thereafter, the tumor volume gradually decreases over a 1-year period. In this study, we prospectively analyzed the frequency and degree of transient expansion, and the relationships between tumor expansion and cranial neuropathies are discussed.

Abbreviations used in this paper: GKS = Gamma Knife surgery; SRS = stereotactic radiosurgery; VS = vestibular schwannoma.

Methods

Patient Population

One hundred consecutive patients with unilateral VS treated with GKS at Chiba Cardiovascular Center between 1998 and 2006 were analyzed in this study. Patient characteristics are shown in Table 1, and radiosurgical parameters in Table 2. There were 32 men and 68 women, with a mean age of 59.1 years (median 59 years, range 29–80 years). Thirty-five patients (35%) had undergone resection.

The SRS was performed using the standard GKS technique.[11,12] The procedure begins with the patient's head being placed in a rigid fixation Leksell G stereotactic frame (Elekta Instruments) after induction of local anesthesia with adequate sedation. Treatment planning was performed using the Leksell Gamma Plan by one

TABLE 1

Characteristics of 100 patients who underwent GKS treatment for VS

Variable	Value
age in yrs	
range	29–80
mean (median)	59.1 (59)
sex (no.)	
male	32
female	68
tumor laterality (no.)	
lt	46
rt	54
no. w/ previous op	35
follow-up period in mos	
range	25–100
mean (median)	65 (66)

neurosurgeon (T.S.) in all cases. For dose planning, we always use contrast-enhanced T1-weighted gradient-echo axial MR sequences (TR 45 msec, TE 3.5 msec, flip angle 30, field of view 260 mm, slice thickness 2 mm, interslice gap 0 mm, and matrix 400 × 382), as well as continuous-interference steady-state sequences and CT scanning. All patients were treated using the Gamma Knife model B (Elekta Instruments). The multiple-isocenter technique was used and the standard prescription dose was 50% 12 Gy in the periphery.

Follow-up neuroimaging included contrast-enhanced T1-weighted gradient-echo MR sequences, the same as those used for dose planning. For each lesion the Gd-enhanced volume was measured serially every 3 months during the 1st year, and 6 months thereafter, using non-invasive volumetric software (GammaPlan or SurgiPlan). The volume measurements were performed by 2 neurosurgeons (T.S. and O.N.). Error was estimated to be < 5%, as verified by phantom studies at another site.[1] We found the margin of error with this method to be ± 5% for lesions in our phantom studies (data not shown). Significant tumor expansion was defined as > 10% enlargement. We defined transient expansion as at least a 10% increase in tumor volume, after SRS, followed by shrinkage. Concurrent neurological deterioration, involving trigeminal, facial, and cochlear nerve functions, was also examined with radiological follow-up by one neurosurgeon (T.S.).

TABLE 2

Radiosurgical parameters in 100 patients with VSs treated with GKS

Variable	Value
tumor vol in cm^3	
range	0.1–13.2
mean (median)	2.7 (2.0)
peripheral dose in Gy	
range	10.5–13.0
mean (median)	12.2 (12.0)
Paddick conformity index	
range	0.43–0.93
mean (median)	0.80 (0.86)
dose rate in Gy/min	
range	1.66–3.67
mean (median)	2.67 (2.73)

Trigeminal neuropathy was defined as any facial dysesthesia within the ipsilateral trigeminal nerve distribution. Facial neuropathy was defined as any deterioration in House–Brackmann facial nerve grade.[7] Acoustic neuropathy was defined as any decline in Gardner–Robertson hearing class[5] for patients with at least Class IV hearing.

The frequency and degree of tumor expansion were documented. The interval between peak expansion and shrinkage to the initial size was analyzed using the Kaplan–Meier method. To analyze prognostic factors, we assessed the following dichotomized variables: age (< 60 vs ≥ 60 years), sex (male vs female), tumor laterality (right vs left), previous surgery (yes vs no), tumor volume (< 2 vs ≥ 2 cm^3), peripheral dose (< 12 vs ≥ 12 Gy), Paddick conformity index[16] (< 0.8 vs ≥ 0.8), and dose rate (< 3.5 vs ≥ 3.5 Gy/min). Factors affecting tumor expansion were evaluated using a logistic regression model. We compared the onsets of these neurological deteriorations between patients with < 30% versus ≥ 30% increment in tumor volume by using the log-rank test. A probability value of < 0.05 was defined as statistically significant.

Results

Radiosurgical Techniques

The tumor volume at GKS averaged 2.7 cm^3 (median 2, range 0.1–13.2 cm^3). The mean peripheral dose was 12.2 Gy (median 12 Gy, range 10.5–13 Gy). The isodose line for the tumor margin varied from 50 to 67% (mean 52.2%, median 50%). Isocenter numbers were 4–42 (mean 16.7, median 17) and the mean Paddick conformity index was 0.80 (range 0.43–0.93).[16] The mean observation period was 65 months (median 66, range 25–100 months).

Maximum tumor expansion rates are shown in Fig. 1. The volume increase was < 10% (no significant increase) in 26 cases, 10–30% in 23, 30–50% in 22, 50–100% in 16, and > 100% in 13. Peak expansion was most frequently observed at 6.4 months after GKS and averaged 47% (range 0–613%) of the initial volume (Fig. 2). Figure 3 demonstrates tumor shrinkage to the initial size. Half the tumors regressed to their initial size within 1 year. Nine percent of tumors were still larger than they had been initially as long as 5 years after treatment. These patients experienced transient expansion, but the tumor remained

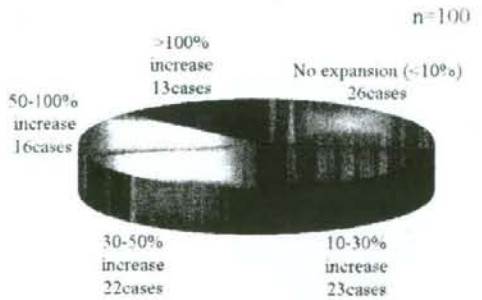

FIG. 1. Pie chart demonstrating the frequency of maximum transient tumor expansion. Volume increases > 100% were seen in 13 patients.

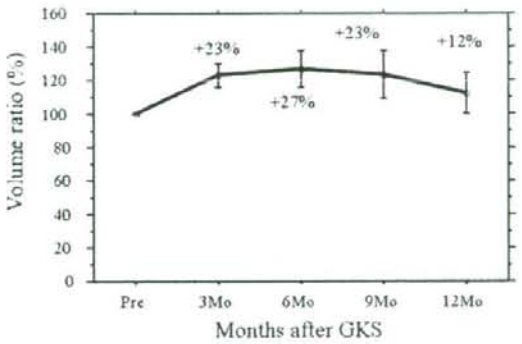

FIG. 2. Graph depicting changes in tumor volume ratios in 100 patients. Tumor volume was increased by 27% at 6 months but had decreased to the initial volume by 18 months postoperatively.

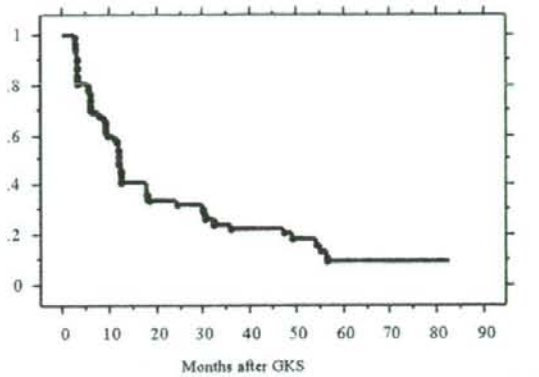

FIG. 3. A Kaplan–Meier curve showing shrinkage to the initial tumor volume in 100 patients. The median survival period was 11.9 months. Nine percent of tumors remained enlarged as long as 5 years after treatment. Values on the y axis denote the tumor shrinkage rate.

larger than the initial volume during follow-up. Tumor volume changes according to age, sex, laterality, previous surgery, tumor volume, peripheral dose, conformity index, and dose rate are presented in Fig. 4. A high dose rate appears to be the greatest risk factor for tumor expansion, but logistic regression did not reveal a statistically significant difference ($p = 0.877$).

There were statistically significant differences in the incidences of trigeminal, facial, and cochlear nerve dysfunctions between patients with tumor expansion < 30% versus ≥ 30% (Fig. 5). Facial dysesthesia was triggered by the tumor attaching to the trigeminal nerve. All MR images of 17 patients with trigeminal neuropathy showed tumor tissue attached to the trigeminal nerve before or after treatment, and in 7 patients this tissue subsequently detached from the trigeminal nerve as the tumor shrank. Improvement of trigeminal neuropathy required a few months after the tumor had been detached from the trigeminal nerve. Twenty patients experienced facial paresis as tumor volume increased. The most common problem of this type was facial spasm (17 patients; 85%). In this study, all patients with facial palsy showed rapid and full recovery to their pre-GKS status, as the tumor shrank. Hearing was preserved in 60% of 28 patients with useful hearing. Half of hearing loss corresponded to tumor expansion, but hearing seldom normalized as the tumor shrank (only 1 patient experienced recovery). The incidence of radiation-induced edema of the cerebellum was 14% in our study. This occurred ~ 6 months after irradiation, corresponding to transient expansion, and decreased as the tumor shrank.

Illustrative Case

This 64-year-old woman had an expanding residual VS after 2 operations. The tumor (3.8 cm^3) was treated with a peripheral dose of 50% 12 Gy (Fig. 6A). The lesion then gradually increased in size (Fig. 6B and C). Nine months after treatment, she experienced facial spasm (House–Brackmann Grade III) and dysesthesia. Admission MR imaging demonstrated that the tumor had doubled in size and showed central low intensity (Fig. 6D). Fifteen months after GKS, expansion was maximal. The tumor was nearly 4 times its original size (Fig. 6E). Thereafter, the tumor shrank to its initial size (Fig. 6G). The patient recovered from the facial paresis as the tumor regressed over a 2-year period, and facial dysesthesia had nearly disappeared 3 years after GKS.

Discussion

Incidences of transient tumor expansion reportedly range from 17 to 62%.[6,14,20,23,24] In contrast, in this study we found that 74% of patients with VS after GKS show significant transient tumor expansion (≥ 10% increase). This difference is attributable to differing observation periods, measurement methods, and cutoff values. We evaluated tumor volumes using MR imaging every 3 months after GKS with 3D measurements based on GammaPlan or SurgiPlan. In most previous reports, tumor volumes were measured by 2D methods with follow-up imaging at 6 months.[6,14,23] This difference indicates that 2D measurement is not suitable for detecting small changes in volume. For example, a 10% increase in diameter is equivalent to a 33% volume expansion.

We found the incidence of transient expansion, with peak expansion usually being observed at 6–9 months, to represent a volume increase to nearly 50% of the initial volume. Irradiation did induce biological changes in the tumors. We did not clarify the mechanism of transient tumor expansion in this study. Several authors have suggested that increased tumor size after GKS could be caused by radiation-induced tumor necrosis,[20] chronic intratumoral bleeding resulting from delayed radiation injury,[8] and/or a biological response to radiation.[14]

Cranial Nerve Dysfunctions

Recently, there have been several reports on transient expansion after SRS for VS, but little is known about neurological deterioration associated with this phenomenon. In the early 1990s, facial nerve paresis after SRS was

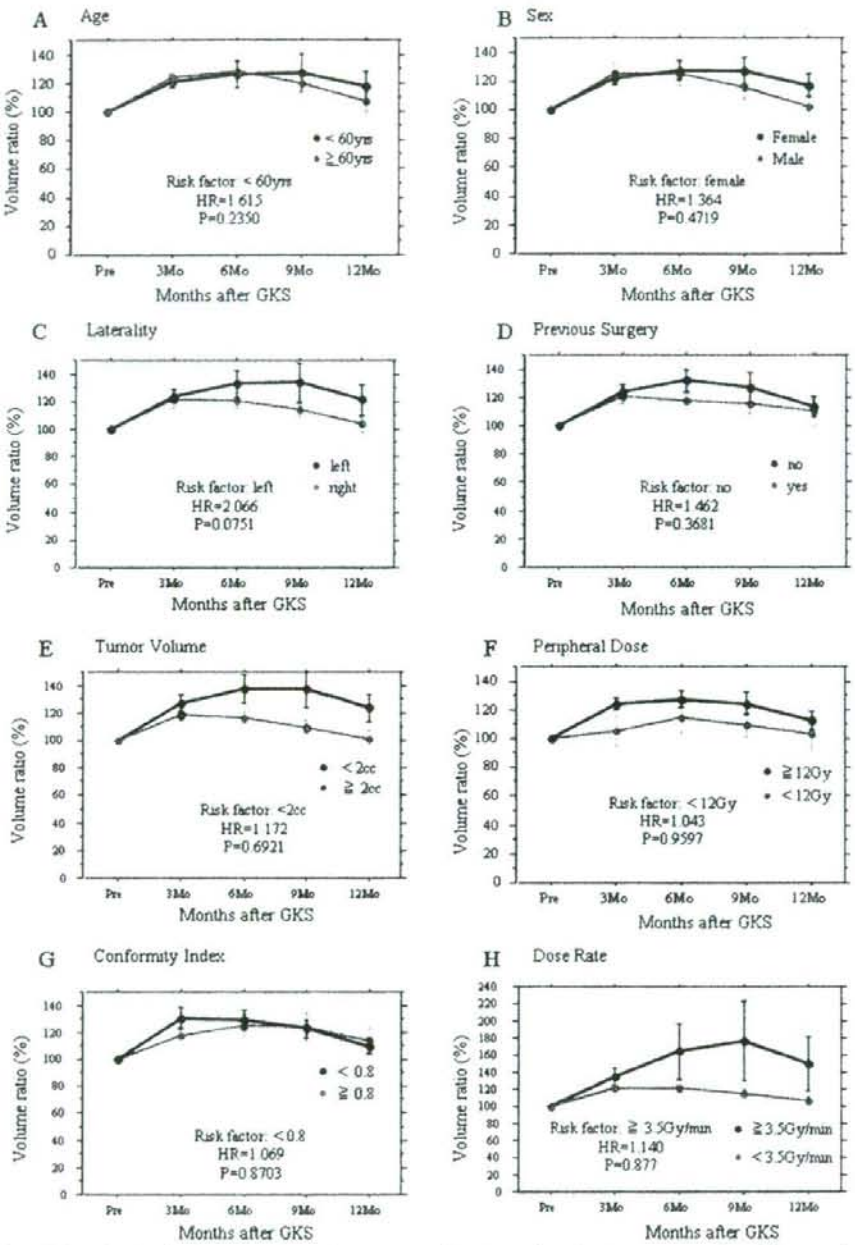

FIG. 4. Graphs showing tumor volume changes according to various factors: age, sex, laterality, previous surgery, tumor volume, peripheral dose, conformity index, and dose rate. A high dose rate seems to be the greatest risk factor for transient expansion. However, logistic regression failed to detect any statistically significant difference. HR = hazard ratio.

considered to result directly from radiation injury, and the treatment dose was thus reduced from 15 Gy to the present 12–13 Gy.[3,17,22] The use of MR imaging for dose planning, combined with CT scanning and improved dose-planning software, has greatly reduced direct radiation injury.[13,15,17] Despite these advances, transient facial spasm does occasionally manifest within 1 year after SRS. In our institute, under close observation, we found that 20% of patients

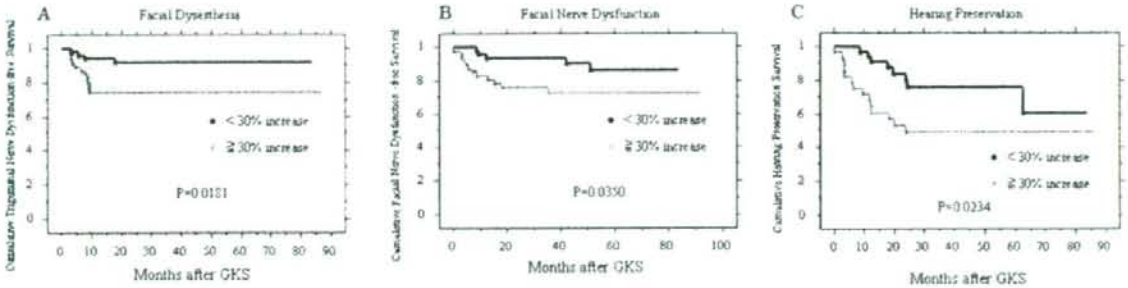

FIG. 5. Kaplan–Meier curves demonstrating the cranial neuropathy-free survival rate based on facial dysesthesia, facial nerve dysfunction, and hearing preservation, comparing patients with a < 30% increase to those with a ≥ 30% increase in tumor volume. The differences are statistically significant.

experienced facial spasm and that it was associated with transient tumor expansion (Fig. 5B). Facial spasm usually started with the lower eyelid, and then extended to the angle of the mouth. This spasm is a temporary phenomenon related to facial paresis, which has been described as facial myokymia.[9,10] The facial spasm disappears as the tumor shrinks.

Trigeminal nerve dysfunction was also strongly related to transient tumor expansion (Fig. 5A). The trigeminal nerve disturbance usually manifested as ipsilateral facial dysesthesia without motor paresis. Patients described the sensation as like anesthesia for a dental procedure or as a pins-and-needles sensation, and typical trigeminal neuralgia was occasionally recognized. This symptom improved as the tumor shrank. However, trigeminal dysesthesia usually improved later than facial paresis, often taking several months or even years to resolve. It is important to inform patients thoroughly about these potential sequelae. Furthermore, we explain to our patients the temporal relationship between transient expansion and these symptoms.

On the other hand, half of hearing loss is attributable to post-GKS deterioration, which is not related to tumor expansion (Fig. 5C). This observation suggests that acoustic nerves may be injured with even lower doses than for the fifth and seventh cranial nerves.[2] However, only 1 of our patients experienced hearing loss after GKS; this patient's hearing normalized as the tumor shrank. To

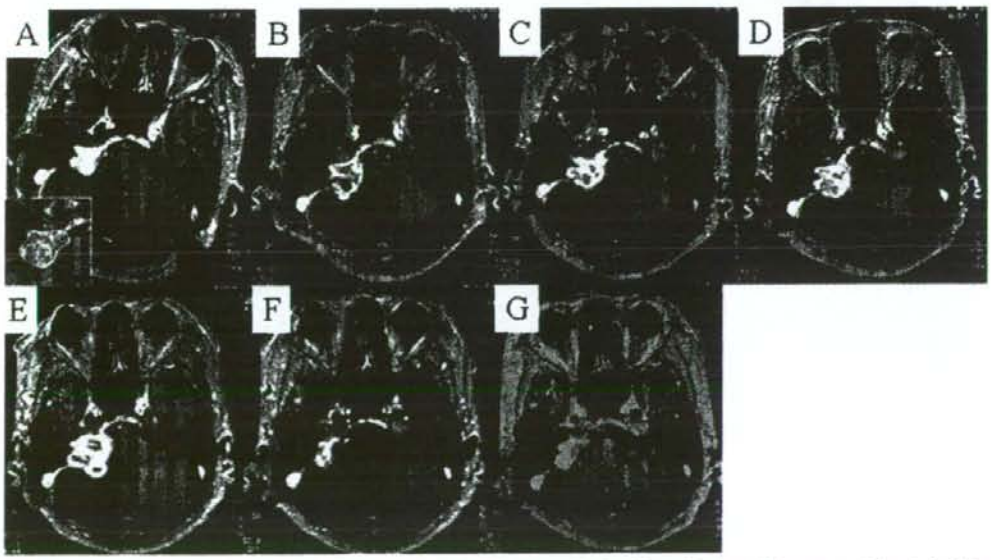

FIG. 6. Serial contrast-enhanced axial T1-weighted MR images obtained in a 64-year-old woman with a right VS who underwent GKS. A: Dose-planning image for a right-sided VS. *Line (inset)* indicates the 50% isodose curve. The initial tumor volume was 3.8 cm^3. B: On an MR image obtained 3 months later, there was an 81% expansion (6.9 cm^3) with central low intensity. C: Image obtained 6 months post-GKS, demonstrating a 97% expansion (7.5 cm^3). D: Image obtained 9 months post-GKS, showing a 105% expansion (7.8 cm^3). E: Image obtained 15 months post-GKS, demonstrating maximum expansion (276%, 14.3 cm^3). F: Image obtained 4 years post-GKS, showing shrinkage to nearly the initial size (3.7 cm^3). G: Image obtained 6 years post-GKS, showing remarkable tumor regression (3.1 cm^3).

preserve hearing, we focused on avoiding high-dose irradiation to the acoustic and/or cochlear nerve during dose planning.

Our analyses suggested that high-dose treatments (≥ 3.5 Gy/min) apparently carry the greatest risk of transient tumor expansion ($p = 0.877$), but the difference was not statistically significant. Additional follow-up of patients with VS will allow us to draw a more definitive conclusion regarding risk factors associated with transient tumor expansion after GKS.

Conclusions

Transient expansion after GKS for VS was found to be much more frequent than previously reported, strongly suggesting a correlation with deterioration of facial and trigeminal nerve functions. However, the present study revealed neither prognostic factors influencing this phenomenon nor the underlying mechanisms.

Disclaimer

The authors report no conflict of interest concerning the materials or methods used in this study or the findings specified in this paper.

Acknowledgment

We thank Bierta E. Barfod, M.D., for her assistance in the preparation of the manuscript.

References

1. Cheung JY, Yu CP, Ho RT: 'Tweaked' GammaPlan for target volume measurement in non-fiducial based images: a simple routine for follow-up assessment. **Stereotact Funct Neurosurg 70 (1 Suppl):**243–248, 1998
2. Flickinger JC, Kondziolka D, Lunsford LD: Dose and diameter relationships for facial, trigeminal, and acoustic neuropathies following acoustic neuroma radiosurgery. **Radiother Oncol 41:**215–219, 1996
3. Flickinger JC, Kondziolka D, Niranjan A, Maitz A, Voynov G, Lunsford LD: Acoustic neuroma radiosurgery with marginal tumor doses of 12 to 13 Gy. **Int J Radiat Oncol Biol Phys 60:**225–230, 2004
4. Fukuoka S, Oka K, Seo Y, Tokanoshi M, Sumi Y, Nakamura H, et al: Apoptosis following gamma knife radiosurgery in a case of acoustic schwannoma. **Stereotact Funct Neurosurg 70 (1 Suppl):**88–94, 1998
5. Gardner G, Robertson JH: Hearing preservation in unilateral acoustic neuroma surgery. **Ann Otol Rhinol Laryngol 97:** 55–66, 1998
6. Hasegawa T, Kida Y, Yoshimoto M, Koike J, Goto K: Evaluation of tumor expansion after stereotactic radiosurgery in patients harboring vestibular schwannomas. **Neurosurgery 58:**1119–1128, 2006
7. House JW, Brackmann DE: Facial nerve grading system. **Otolaryngol Head Neck Surg 93:**146–147, 1985
8. Iwai Y, Yamanaka K, Yamagata K, Yasui T: Surgery after radiosurgery for acoustic neuromas: surgical strategy and histological findings. **Neurosurgery 60 (2 Suppl):**ONS75–ONS82, 2007
9. Joseph BV, Rajshekhar V: Facial myokymia as a presenting symptom of vestibular schwannoma. **Neurol India 50:**369–370, 2002
10. Kiriyanthan G, Krauss JK, Glocker FX, Scheremet R: Facial myokymia due to acoustic neurinoma. **Surg Neurol 41:** 498–501, 1994
11. Kondziolka D, Lunsford LD, McLaughlin MR, Flickinger JC: Long-term outcomes after radiosurgery for acoustic neuromas. **N Engl J Med 339:**1426–1433, 1998
12. Lunsford LD, Niranjan A, Flickinger JC, Maitz A, Kondziolka D: Radiosurgery of vestibular schwannomas: summary of experience in 829 cases. **J Neurosurg 102 (Suppl):**195–199, 2005
13. Miller RC, Foote RL, Coffey RJ, Sargent DJ, Gorman DA, Schomberg PJ, et al: Decrease in cranial nerve complications after radiosurgery for acoustic neuromas: a prospective study of dose and volume. **Int J Radiat Oncol Biol Phys 43:**305–311, 1999
14. Nakamura H, Jokura H, Takahashi K, Boku N, Akabane A, Yoshimoto T: Serial follow-up MR imaging after gamma knife radiosurgery for vestibular schwannoma. **AJNR Am J Neuroradiol 21:**1540–1546, 2000
15. Niranjan A, Lunsford LD, Flickinger JC, Maitz A, Kondziolka D: Dose reduction improves hearing preservation rates after intracanalicular acoustic tumor radiosurgery. **Neurosurgery 45:**753–762, 1999
16. Paddick I: A simple scoring ratio to index the conformity of radiosurgical treatment plans. Technical note. **J Neurosurg 93 (3 Suppl):**219–222, 2000
17. Petit JH, Hudes RS, Chen TT, Eisenberg HM, Simard JM, Chin LS: Reduced-dose radiosurgery for vestibular schwannomas. **Neurosurgery 49:**1299–1306, 2001
18. Pollock BE: Management of vestibular schwannomas that enlarge after stereotactic radiosurgery: treatment recommendations based on a 15 year experience. **Neurosurgery 58:**241–248, 2006
19. Pollock BE, Lunsford LD, Kondziolka D, Sekula R, Subach BR, Foote RL, et al: Vestibular schwannoma management. Part II. Failed radiosurgery and the role of delayed microsurgery. **J Neurosurg 89:**949–955, 1998
20. Prasad D, Steiner M, Steiner L: Gamma surgery for vestibular schwannoma. **J Neurosurg 92:**745–759, 2000
21. Unger F, Walch C, Schröttner O, Eustacchio S, Sutter B, Pendl G: Cranial nerve preservation after radiosurgery of vestibular schwannomas. **Acta Neurochir Suppl 84:**77–83, 2002
22. van Eck AT, Horstmann GA: Increased preservation of functional hearing after gamma knife surgery for vestibular schwannoma. **J Neurosurg 102 (Suppl):**204–206, 2005
23. Wowra B, Muacevic A, Jess-Hempen A, Hempel JM, Muller-Schunk S, Tonn JC: Outpatient gamma knife surgery for vestibular schwannoma: definition of the therapeutic profile based on a 10-year experience. **J Neurosurg 102 (Suppl):**114–118, 2005
24. Yu CP, Cheung JY, Leung S, Ho R: Sequential volume mapping for confirmation of negative growth in vestibular schwannomas treated by gamma knife radiosurgery. **J Neurosurg 93 (3 Suppl):**82–89, 2000

Manuscript submitted July 10, 2007.
Accepted December 17, 2007.

Address correspondence to: Osamu Nagano, M.D., Department of Neurological Surgery, Chiba University, Graduate School of Medicine, 1-8-1 Inohana, Chuou-ku, Chiba City, Chiba, 2600856, Japan. email: osamu5@xk9.so-net.ne.jp.

Association of p16 Homozygous Deletions with Clinicopathologic Characteristics and EGFR/KRAS/p53 Mutations in Lung Adenocarcinoma

Reika Iwakawa,[1,6] Takashi Kohno,[1] Yoichi Anami,[4] Masayuki Noguchi,[4] Kenji Suzuki,[2] Yoshihiro Matsuno,[3] Kazuhiko Mishima,[5] Ryo Nishikawa,[5] Fumio Tashiro,[6] and Jun Yokota[1]

Abstract **Purpose:** The *p16* gene is frequently inactivated in lung adenocarcinoma. In particular, homozygous deletions (HD) have been frequently detected in cell lines; however, their frequency and specificity is not well-established in primary tumors. The purpose of this study was to elucidate the prevalence and the timing for the occurrence of p16 HDs in lung adenocarcinoma progression *in vivo*.

Experimental Design: Multiple ligation-dependent probe amplification was used for the detection of p16 HDs in 28 primary small-sized lung adenocarcinomas and 22 metastatic lung adenocarcinomas to the brain. Cancer cells were isolated from primary adenocarcinoma specimens by laser capture microdissection. HDs were confirmed by quantitative real-time genomic PCR analysis.

Results: HDs were detected in 8 of 28 (29%) primary tumors, including 2 of 8 (25%) noninvasive bronchioloalveolar carcinomas, and 5 of 22 (26%) brain metastases, respectively. No significant associations were observed between p16 HDs and gender, age, smoking history, stage, and prognosis. HDs were detected with similar frequencies (17–29%) among adenocarcinomas with epidermal growth factor receptor (EGFR) mutations, with KRAS mutations, and without EGFR/KRAS mutations, and with similar frequencies (22–28%) between adenocarcinomas with and without p53 mutations.

Conclusions: p16 HDs occur early in the development of lung adenocarcinomas and with similar frequencies among EGFR type, KRAS type, and non-EGFR/KRAS type lung adenocarcinomas. Tobacco carcinogens would not be a major factor inducing p16 HDs in lung adenocarcinoma progression.

Adenocarcinoma is the most common histologic type of lung cancer. Recent molecular analyses have indicated that lung adenocarcinoma can be divided into at least three types; the epidermal growth factor receptor (EGFR) type, the KRAS type, and the non-EGFR/KRAS type, based on accumulated genetic alterations in adenocarcinoma cells (1, 2). The *p16* tumor suppressor gene is frequently inactivated in lung adenocarcinomas, most prominently through promoter methylation and homozygous deletion (HD), and less frequently through intragenic mutation (3–6). In particular, p16 methylation is known to occur in close association with tobacco carcinogen exposure and preferentially in the KRAS type adenocarcinomas (1). Molecular analyses of small-sized adenocarcinomas revealed that p16 methylation occurs in the course of progression from noninvasive bronchioloalveolar carcinomas (BAC) to invasive ones, and its occurrence is associated with smoking history, staging, and prognosis (7). However, it is still unknown whether p16 HD also occurs preferentially in the KRAS type or not. In addition, the involvement of tobacco smoking in the occurrence of p16 HD is also unclear because both positive and negative associations between tobacco smoking and HD have been reported (5, 6). Indeed, p16 HDs have been reported to occur with a highly variable frequency in primary lung adenocarcinomas (0–40%; refs. 3–6, 8). HD can be easily masked if a large fraction of noncancerous cells are contaminated in tumor tissues, in particular, in the analysis of small tumors with a BAC component. Thus, such an inconsistency could come not only from the diversity and/or heterogeneity of lung adenocarcinomas but also from tumor tissues used for the analysis and also from the methods used for the detection of HDs. For instance, immunohistochemical analyses of p16 proteins have shown that a considerable

Authors' Affiliations: [1]Biology Division, National Cancer Center Research Institute, [2]Thoracic Surgery Division and [3]Diagnostic Pathology Division, National Cancer Center Hospital, Tokyo, Japan; [4]Department of Pathology, Institute of Basic Medical Sciences, Graduate School of Comprehensive Human Sciences, Tsukuba University, Ibaraki, Japan; [5]Department of Neuro-Oncology, Comprehensive Cancer Center, International Medical Center, Saitama Medical University, Saitama, Japan; and [6]Department of Biological Science and Technology, Faculty of Industrial Science and Technology, Tokyo University of Science, Chiba, Japan

Received 10/5/07; revised 2/24/08; accepted 2/28/08.

Grant support: Grants-in-Aid from the Ministry of Health, Labor and Welfare for the Third-Term Comprehensive 10-Year Strategy for Cancer Control and for Cancer Research (16-1) and a Grant-in-Aid for the Program for Promotion of Fundamental Studies in Health Sciences of the National Institute of Biomedical Innovation (NiBio).

The costs of publication of this article were defrayed in part by the payment of page charges. This article must therefore be hereby marked *advertisement* in accordance with 18 U.S.C. Section 1734 solely to indicate this fact.

Requests for reprints: Jun Yokota, Biology Division, National Cancer Center Research Institute, 1-1, Tsukiji 5-chome, Chuo-ku, Tokyo 104-0045, Japan. Phone: 81-33547-5272; Fax: 81-33542-0807; E-mail: jyokota@ncc.go.jp.

doi:10.1158/1078-0432.CCR-07-4552

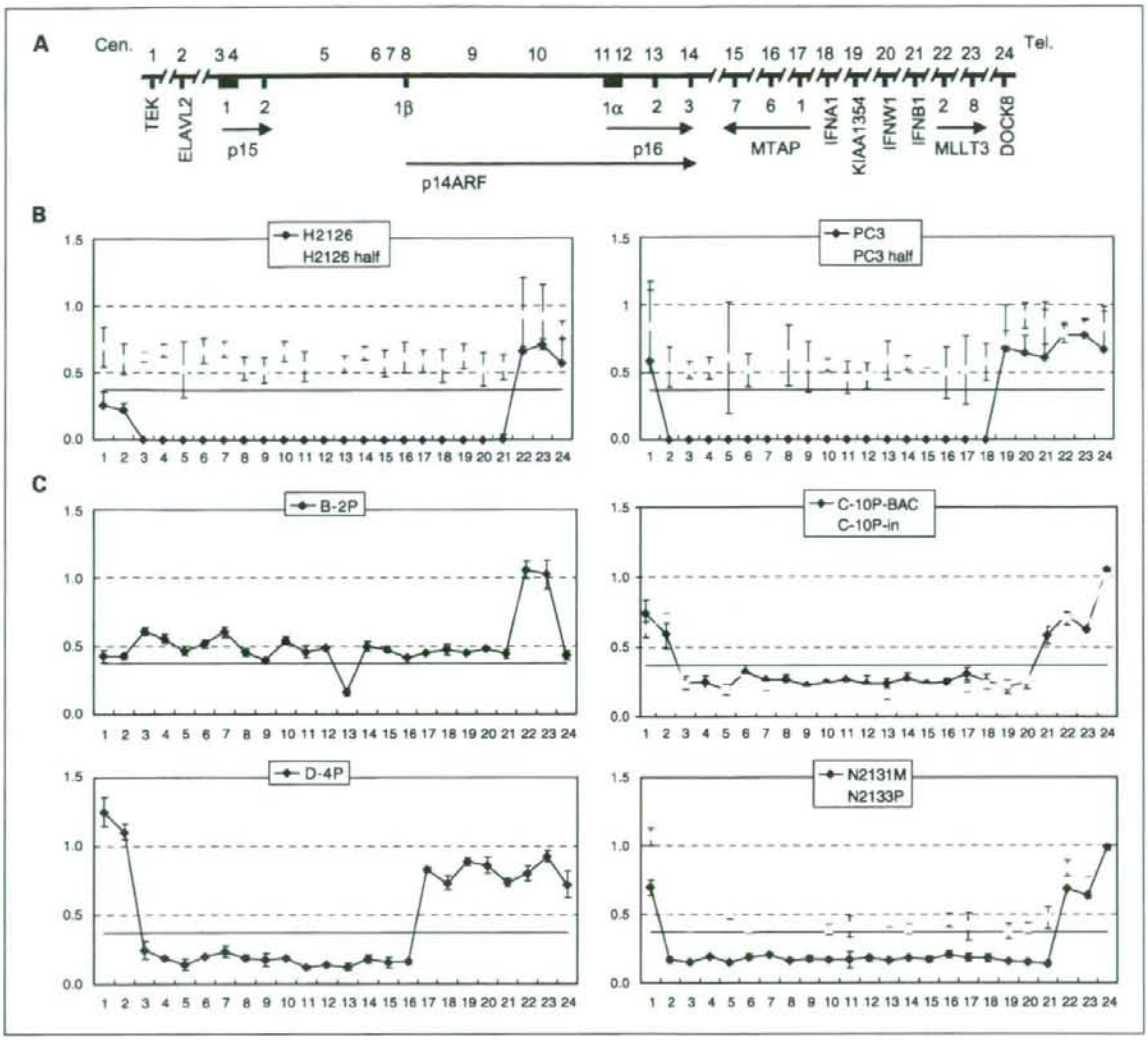

Fig. 1. HDs of the *p16* gene detected by MLPA analysis. *A*, physical map of the chromosome 9p region. Top, positions of 24 probes from nos. 1 to 24 (*red*) in the order from centromere (*Cen.*) to telomere (*Tel.*). Bottom, positions of 12 genes in this region (*light blue*). Exons (*numbers*) and orientations (*arrows*) of the *p15*, *p14ARF*, *p16*, *MTAP*, and *MLLT3* genes. *B*, definition of p16 HDs by MLPA analysis. Relative copy numbers of the 24 loci in two lung adenocarcinoma cell lines, H2126 and PC3 (*blue dots/lines*), and those in mixed samples of the same amounts of DNA from these cell lines and normal lung tissue (*pink dots/lines*; H2126 half and PC3 half, respectively). *C*, results of MLPA analysis for cases B-2P, C-10P, D-4P, and N2131M/N2133P showing HDs of the *p16* gene. As for case C-10P, both the BAC component (*BAC; blue dots/lines*) and the invasive region (*in; pink dots/lines*) of the tumor were analyzed. N2131M (*blue*) and N2133P (*pink*) are a brain metastasis and the primary tumor from the same patient, respectively.

fraction of adenocarcinomas are negative for p16 protein expression without clear evidence of an inactivating event by molecular analyses of the *p16* gene (4, 5, 7). Thus, it has been assumed that p16 HD is a causative event for the absence of p16 protein in these adenocarcinoma cases. However, due to the lack of comprehensive analysis for p16 HDs, the prevalence, specificity, and the timing for the occurrence of p16 HDs in lung adenocarcinoma progression *in vivo* is still unclear.

In this study, we investigated the association of p16 HDs with clinicopathologic characteristics, including smoking history, of lung adenocarcinomas and with the status of EGFR, KRAS, and p53 mutations in lung adenocarcinomas. To obtain more critical information than previous studies for the timing of its occurrence in the progression of lung adenocarcinomas, we analyzed two typical stages of lung adenocarcinomas. One is a primary small-sized adenocarcinoma of ≤2 cm in maximum diameter as a representative of early stage lung adenocarcinomas, and the other is a brain metastasis as a representative of late stage lung adenocarcinomas. To exclude the possible overlooking of HDs in the analysis due to contamination of noncancerous cells in tumor tissues, a laser capture

microdissection method was applied for the isolation of cancer cells from small-sized primary lung adenocarcinomas. Brain metastases are known to be relatively solid and generally contain a small amount of noncancerous cells in tumor tissues; therefore, macrodissected samples were used for the analysis. Recently, a simple and effective method, which is called multiplex ligation-dependent probe amplification (MLPA), to measure the copy number of up to 45 genomic loci in a single experiment, was developed and has been applied for the detection of large deletions in/of various genes in the human genome DNA sequence (9). For instance, this method was successfully applied for the detection of p16 hemizygous deletions in melanoma families (10) and p16 HDs in head and neck squamous cell carcinoma cell lines (11). Thus, we applied this method for the detection of p16 HDs in surgically resected lung adenocarcinomas. HDs were detected with similar frequencies of 23% to 40% in lung adenocarcinomas of any progression stage—from noninvasive carcinomas to advanced ones. The deletions were also detected with similar frequencies among EGFR type, KRAS type, and non-EGFR/KRAS type adenocarcinomas, and were not associated with tobacco smoking and poor prognosis.

Materials and Methods

Patients and tissues. Twenty-eight primary small-sized (≤2 cm in maximum diameter) adenocarcinomas, 22 brain metastases, and corresponding noncancerous tissues were obtained at surgery from lung adenocarcinoma patients treated at the National Cancer Center Hospital, Tokyo and at the Saitama Medical University. In 4 of the 22 brain metastasis cases, the corresponding primary tumors were also obtained at surgery. The surgically resected specimens were fixed routinely with 10% formalin and embedded in paraffin for histologic examination. All the sections were stained with H&E and examined by light microscopy. The tumors were pathologically diagnosed according to the tumor-node-metastasis classification of malignant tumors (12). The primary small-sized adenocarcinomas were further classified into three types according to the histologic classification of small-sized adenocarcinoma of the lung reported by Noguchi and colleagues (13), and there were 8 type B, 15 type C, and 5 type D adenocarcinomas. These 28 tumors and corresponding noncancerous tissues were fixed with methanol and embedded in paraffin. Cancer cells were then microdissected using the Pixcell Laser Capture Microdissection system (Arcturus Engineering), and their genomic DNAs were extracted as described previously (14). Representative figures of type B and C tumors before and after microdissection have been shown in our previous article (14). All of the 22 brain metastases, corresponding primary tumors, and noncancerous tissues were macrodissected and stored at -80°C until DNA extraction. Genomic DNAs were prepared as previously described (15).

Cell lines. Three lung adenocarcinoma cell lines, H2126, A549, and PC3, were used as positive controls of p16 HDs in MLPA and quantitative real-time genomic PCR (QRT-G-PCR) analysis. Genomic DNA were prepared as previously described (15). Incidence as well as regions of p16 HDs in 55 lung adenocarcinoma cell lines, including these three cell lines, were determined by multiplex PCR analysis in our previous studies (3).

MLPA analysis. MLPA was carried out using the P024B kit for the 9p21 CDKN2A/2B region (MRC-Holland) according to the manufacturer's protocol. The kit contains 12 probes covering the *p15/p14ARF/p16* genes, 12 probes for 9 other genes on chromosome 9p, and 15 control probes for nonchromosome 9p loci. Genes on chromosome 9p included in this screen were *TEK, ELAVL2, CDKN2B* (*p15*), *CDKN2A* (*p14ARF/p16*), *MTAP, IFNA1, KIAA1354, IFNW1, IFNB1, MLLT3,* and *DOCK8* (*FLJ00026*) in the order from centromere to telomere (Fig. 1A). Experiments were done in a half volume until the ligation reaction step, and then by the supplied protocol. Briefly, 12.5 to 50 ng of genomic DNA in 2.5 to 5 μL of TE buffer were heat-denatured and hybridized to probes for 16 h at 60°C. The hybridized probes were then ligated and amplified by PCR of 35 cycles at 60°C for 30 s and 72°C for 60 s. PCR products were separated by capillary electrophoresis using the ABI3700 Automated Capillary DNA Sequencer with a 50-cm capillary array, ABI POP-6 polymer, and GeneScan-ROX 500 size standards (Applied Biosystems). Analysis was automated using ABI PRISM GeneScan Analysis software version 3.7, and Genotyper Analysis software version 3.7 (Applied Biosystems). PCR and electrophoresis, respectively, were done in duplicate, and the mean of four values was calculated and considered to be the DNA copy number ratio of each locus.

Data analysis. The relative DNA copy number of each locus was calculated as follows. First, the value for the sum of 15 autosomal control probe peak areas in a lung adenocarcinoma sample was adjusted to the mean value for those in two or three normal lung tissue samples in the same run. Each of the 39 probe peak areas was then divided by the sum of the peak areas of the 15 autosomal control probe peak areas. Finally, the relative DNA copy number ratio of each of the 39 chromosome loci in the lung adenocarcinoma samples against the normal lung tissue samples was calculated. Theoretically, ratios close to 1.0 indicated that two DNA copies were present (i.e., wild-type), a ratio of 0.5 indicated that one copy was absent (i.e., hemizygous deletion), and a ratio of 0.0 indicated that both copies were absent (i.e., homozygous deletion). The criteria for hemizygous deletions and HDs of the 39 loci by MLPA analysis were defined using MLPA data from three lung adenocarcinoma cell lines with p16 HDs as described in Results and Discussion. The *p16* gene was then defined as homozygously deleted or not in each sample. Because the purpose of this study is to evaluate the prevalence of p16 HD, hemizygous deletions were not evaluated from MLPA data.

QRT-G-PCR analysis. TaqMan-MGB probes and primers were designed using Primer Express software (Applied Biosystems) and were optimized according to the manufacturer's guidelines. Target and reference locus probes were labeled with FAM and VIC, respectively. Probe sequences were as follows: no. 9, 5′-AACTCCTCCACTGATTAC-3′; and 2p14, 5′-CCAGCCTATTCCTGC-3′. Primer sequences were as follows: no. 9-F/R, 5′-GGGTCTCCTTCATTTGGTGAAA-3′/5′-GGATCCCAGGGAGGAGAGTCT-3′; and 2p14-F/R, 5′-AAGAAGACTGGAGTGGTGTTTGG-3′/5′-CACAATGCTGAATACTGTCAATGAAA-3′. PCR was carried out in duplicate using 1 ng of DNA as a template. Primer and probe concentrations were optimized for each target according to the manufacturer's instructions. The PCR program consisted of 50°C for 2 min and 95°C for 15 min followed by 45 cycles of 95°C for 15 s and 60°C for 1 min. Standard curves for the copy numbers of the target and reference genes were generated using serially diluted (0.04–25 ng) normal lung tissue DNA. Data analysis was carried out using ABI Prism 7900HT Sequence Detection Software. DNA copy number ratios were calculated as the average copy number of the target locus divided by the average copy number of the reference locus, and then normalized against the normal lung tissue DNA to give a normalized DNA copy number ratio.

Immunohistochemistry. Immunohistochemical analysis of p16 protein was performed as described previously (7) using 4-μm sections cut from methanol-fixed and paraffin-embedded specimens of 28 primary small-sized adenocarcinomas, which were subjected to MLPA analysis. Positivity for p16 staining was scored by the same criteria as previously described (7). In brief, only nuclear staining was scored, and was considered to be positive when it was more intense than the background cytoplasmic staining. If <10% of tumor cells displayed p16 protein staining, it was judged negative; and if >10% of them showed strong staining, it was judged positive.

Mutation analysis of the EGFR, KRAS, and p53 genes. Thirteen of the 28 primary tumors, and 16 of the 22 brain metastases were